Journal of Controlled Release 251 (2017) 82–91

Contents lists available at ScienceDirect

Journal of Controlled Release

journal homepage: www.elsevier.com/locate/jconrel

Aptamer-based liposomes improve specific drug loading and release

Kevin Plourde [a], Rabeb Mouna Derbali [a], Arnaud Desrosiers [b], Céline Dubath [a], Alexis Vallée-Bélisle [b], Jeanne Leblond [a,*]

[a] Faculty of Pharmacy, University of Montreal, QC H3T 1J4, Canada
[b] Department of Chemistry, University of Montreal, QC H3T 1J4, Canada

ARTICLE INFO

Article history:
Received 31 August 2016
Received in revised form 27 January 2017
Accepted 7 February 2017
Available online 24 February 2017

Keywords:
Liposome
Aptamer
Doxorubicin
Encapsulation efficiency
Controlled release
Active loading

ABSTRACT

Aptamer technology has shown much promise in cancer therapeutics for its targeting abilities. However, its potential to improve drug loading and release from nanocarriers has not been thoroughly explored. In this study, we employed drug-binding aptamers to actively load drugs into liposomes. We designed a series of DNA aptamer sequences specific to doxorubicin, displaying multiple binding sites and various binding affinities. The binding ability of aptamers was preserved when incorporated into cationic liposomes, binding up to 15 equivalents of doxorubicin per aptamer, therefore drawing the drug into liposomes. Optimization of the charge and drug/aptamer ratios resulted in ≥80% encapsulation efficiency of doxorubicin, ten times higher than classical passively-encapsulating liposomal formulations and similar to a pH-gradient active loading strategy. In addition, kinetic release profiles and cytotoxicity assay on HeLa cells demonstrated that the release and therapeutic efficacy of liposomal doxorubicin could be controlled by the aptamer's structure. Our results suggest that the aptamer exhibiting a specific intermediate affinity is the best suited to achieve high drug loading while maintaining efficient drug release and therapeutic activity. This strategy was successfully applied to tobramycin, a hydrophilic drug suffering from low encapsulation into liposomes, where its loading was improved six-fold using aptamers. Overall, we demonstrate that aptamers could act, in addition to their targeting properties, as multifunctional excipients for liposomal formulations.

1. Introduction

Aptamer technology, although discovered for 25 years, is still evolving to fulfill the requirements of more precise diagnosis and personalized therapy [1,2]. Aptamers are RNA or DNA sequences generated to exhibit high affinity and specificity against a broad range of targets, ranging from small molecules to whole cells or tissues [2–4]. Like antibodies, they recognize their specific targets due to the unique three-dimensional structure they adopt. Nucleotides aptamers, however, exhibit several improved properties when compared to antibodies, such as lower immunogenicity, higher thermal stability, rapid and large-scale synthesis and lower production costs [5,6]. To date, they have shown a high potential for clinical translation, especially in the field of drug and biomarker discovery [7,8], biosensor design [9,10], vaccines [11] and molecular imaging [12,13].

The pioneering work of Farokhzad et al. first demonstrated the potential of conjugating an aptamer to the surface of polymeric nanoparticles for targeting prostate cancers *in vivo* [14]. Since then, aptamers have been conjugated to multiple nanocarriers to provide specific recognition of biological targets, showing much promise in targeted cancer therapeutics [15,16]. However, loading sufficient therapeutics into nanocarriers, while controlling its release rate in order to reach therapeutic concentrations at the target site, still remains a major limitation of nanocarriers [17–19]. Liposomes, for instance, offer unique benefits for clinical applications, such as large internal volume for high drug loading, prolonged circulation times and controlled biodistribution, as well as excellent biocompatibility and biodegradability [20]. To improve drug loading capacity, current strategies exploit a trans-membrane gradient, such as pH- or ion- gradient, to actively load and retain the drug into the liposomal core [21]. The most successful example is Doxil, commercialized liposomes of doxorubicin, able to reach up to 10,000 molecules of doxorubicin per liposome, most of which existing in the crystalline phase [21]. The liposome formulation significantly reduced the cardiotoxicity of doxorubicin, but the strong entrapment of the drug within the core significantly reduced its release, and, by extension, its therapeutic efficacy [22]. In extreme cases, such as liposomal cisplatin, the therapeutic efficacy has even been abolished [23]. Alternative methods are therefore pursued to provide a better control over the loading and release of the encapsulated drug [24]. Recent studies have used ATP-binding aptamers to selectively release doxorubicin in an ATP-rich environment from nanogels [25,26], graphene nanosheets [27] or cross-linked microcapsules [28]. Aptamer-

* Corresponding author at: PO Box 6128, Downtown Station, Montréal, QC H3C 3J7, Canada.
E-mail address: Jeanne.leblond-chain@umontreal.ca (J. Leblond).

http://dx.doi.org/10.1016/j.jconrel.2017.02.026
0168-3659/

functionalized hydrogels have also been programmed to release various and multiple therapeutics when needed through specific nucleic acid recognition and complementary hybridization process [29,30].

In this study, we propose to use drug-specific aptamers to improve drug loading into liposomes. Indeed, specific aptamers have been designed to show a tunable affinity for a variety of drugs such as doxorubicin [31,32], cocaine [33] or neomycin [34]. Interestingly, the loading and release rate of the drug from aptamer-drug complexes is a function of the sequence [32,34] and the number of binding sites [31]. However, these complexes suffer from a low stability in the blood, limited drug loading capacity and some inherent immunogenicity of the aptamers [15,35]. We hypothesize that incorporating the drug-aptamer complex into liposomes will improve specific drug loading and offer a better control over the release rate to improve the therapeutic efficiency. We have designed specific aptamer sequences to tune the binding affinity of doxorubicin and incorporated them into liposomal formulations. The impact on drug loading, drug release and therapeutic efficacy was investigated. This proof-of-concept was first demonstrated with doxorubicin and applied to tobramycin, a hydrophilic drug suffering from low encapsulation into liposomes.

2. Material and methods

2.1. Chemicals and material

All lipids were purchased from Avanti Polar Lipids (Alabaster, AL). DNA aptamers and control nucleotide sequences were purchased from Sigma-Aldrich custom oligonucleotide synthesis service (Oakville, ON). The sequences are detailed in Table S1. Doxorubicin hydrochloride was purchased from Sigma-Aldrich and tobramycin sulphate was purchased from AK Scientific (CA, USA). EMEM (ATCC® 30-2003™), PBS and TrypLE Express was purchased from GE Healthcare (Baie-d'Urfé, QC). All sterile consumables were purchased from Sarstedt (Montreal, QC). All reagents, solvents and salts were either purchased from Sigma-Aldrich (Oakville, ON) or Fisher Scientific (Whitby, ON). HeLa cells (ATCC® CCL-2™) were kindly provided by Prof. Marc Servant (University of Montreal).

2.2. Dissociation constants of aptamer-doxorubicin complexes

Dissociation constants for the different aptamer-doxorubicin complexes were obtained by monitoring the quenching of doxorubicin fluorescence at various aptamer concentrations. DNA aptamer solution (0.1 mM in a solution of 5% dextrose and 5 mM NaCl) was denatured 5 min at 95 °C, vortexed for 1 min and annealed at room temperature. Doxorubicin sample concentration was kept constant in all samples (100 nM in 5% dextrose and 5 mM NaCl). Fluorescence emission spectrum (λ_{ex} 485 nm, λ_{em} 520–700 nm) was recorded at 37 °C on a Cary Eclipse Fluorescence spectrophotometer (Agilent Technologies, Mississauga, ON). Increasing amounts of DNA were added and equilibrated 1 min at 37 °C in the same cuvette, producing DNA concentrations ranging from 0.001 to 25 μM with incrementing volumes <20% of final volume. Emission scans were taken at a high resolution of 100 nm/min and data were smoothed with a 10-neighbors Savitzky-Golay factor. The area under curve of the full scan was considered for the analysis. The dissociation constant (K_D, nM) was calculated using GraphPad Prism 6 with the equation $Y = M_1 + (M_2 * X) / (X + M_3)$, where M_1 is the initial value of Y, M_2 is its magnitude and M_3 is the K_D. In the definition of Poly-Doxapt concentrations, one strand A complexed with one strand A′ was considered as one aptamer molecule (two binding sites).

2.3. Preparation and characterization of liposomes

All liposome formulations, except Doxil-like, were prepared using the hydration method. Briefly, stock solutions of lipids in chloroform (20–40 mg/mL) were stored under argon at −80 °C before use. For the preparation of cationic liposomes, 1,2-dioleoyl-3-trimethylammonium-propane (DOTAP), cholesterol and 1,2-distearoyl-*sn*-glycero-3-phosphoethanolamine-*N*-(polyethylene glycol)-2000 (DSPE-PEG_{2000}) solutions were combined in a 10-mL round bottom flask in a 50/48/2 molar ratio to get 30 μmol total lipid amount. The solvent was evaporated under reduced pressure at 50 °C. The dried lipid film was hydrated 30 min at 60 rpm with 1 mL of 5% dextrose and 5 mM NaCl. "No cationic lipid" formulation consisted in 1-palmitoyl-2-oleoyl-*sn*-glycero-3-phosphocholine (POPC), cholesterol and DSPE-PEG_{2000} in a 55/40/5 molar ratio. All liposomes were extruded through 400 and 200 nm polycarbonate membranes using a LiposoFast manual extruder (Avestin Inc., Ottawa, ON, Canada) at room temperature. Doxil-like liposomes were prepared following the same procedure with minor modifications. Lipid composition was 55% 1,2-distearoyl-*sn*-glycero-3-phosphocholine (DSPC), 40% cholesterol and 5% DSPE-PEG_{2000} (10 μmol total lipid amount). The dried lipid film was hydrated 30 min at 65 °C (60 rpm) with 1 mL of a 120 mM ammonium sulphate salt solution. Extrusion was performed at controlled temperature (65 °C) to ensure the fluidity of the lipids, using a homemade heating block for the manual extruder. Finally, Doxil-like liposomes were purified on a 1 × 20 cm Sephadex G-50 (medium) column equilibrated in a pH 7.4 buffer (5 mM Tris and 145 mM NaCl) to exchange external medium. All liposome preparations (total final volume ~ 2 mL) were stored in darkness at 4 °C in 4 mL glass vials.

Liposome hydrodynamic diameter and ζ-potential were measured at 25 °C using a Malvern Zetasizer Nano ZS (Malvern, Worcestershire, UK) using the automatic algorithm mode at a scattering angle of 173°. Size measurements, reported in intensity, were performed in a pH 7.4 buffer (5 mM Tris and 145 mM NaCl). ζ-Potential measurements were obtained using the Smoluchowski model by diluting the liposome sample in MilliQ purified water, using 0.1 mM total lipid concentration in the cuvette. Experiments were run in triplicates or more.

2.4. Preparation of aptamer-loaded lipoplexes

Aptamer spiking solution (5% dextrose and 5 mM NaCl) was denatured 5 min at 95 °C, vortexed for 1 min and annealed at room temperature. Aptamer solution was then added dropwise under stirring into 2.5 mM liposomal solution (1:1 v/v) at predefined N/P ratios (0.5–15). N is the number of amines (molar quantity of DOTAP) and P is the number of phosphorous groups of aptamers (corresponding to the number of nucleotides). Lipoplexes were incubated in a VorTemp 56 (Labnet, Edison, NJ) for 25 min, at 1000 rpm and 30 °C. Lipoplexes (total final volume ~ 1 mL) were immediately used after incubation to determine the encapsulation efficiency of aptamers. N/P ratio was optimized for each formulation to encapsulate >90% of aptamers so that no further removal of unencapsulated aptamer was required.

2.5. Encapsulation efficiency of aptamers

Two methods were used to determine the encapsulation efficiency of aptamers into cationic liposomes. Through the indirect method, the residual aptamer concentration in solution (1–150 nM) was quantified using fluorescent intercalating probes SYBRGold or SYBRGreen (Thermo Scientific) for Apt-Ctrl-2 or all other aptamers, respectively. An aliquot of lipoplexes was diluted to 300 μL in 5% dextrose and 5 mM NaCl and centrifuged 60 min at 18,500*g* at room temperature. The supernatant was diluted to fit in the linear range (1–150 nM) and SYBRGreen 100× (or SYBRGold for Apt-Ctrl-2) was added (5% total volume). 150 μL of each sample was added to a 96-well plate and analyzed with a Safire microplate reader (Tecan, Männedorf, Switzerland) (λ_{exc} 496 nm, λ_{em} 523 nm for both SYBRGreen and SYBRGold). A calibration curve was determined for each DNA sequence. The amount of free DNA

was determined and the encapsulation efficiency was calculated using Eq. (1).

$$\text{EE}\ (\%) = \frac{\text{Total DNA} - \text{Free DNA}}{\text{Total DNA}} * 100\% \quad (1)$$

In addition, the amount of encapsulated aptamers within the lipoplexes was quantified directly according to a second fluorescent assay. 2 mL of a solution of 1× SYBRGreen (or SYBRGold) in 5% dextrose and 5 mM NaCl was placed in a 3 mL cuvette. The fluorescence of this solution was monitored over time on a F-2710 Spectrophotometer (Hitachi High Technologies America Inc., Schaumburg, IL, USA) at wavelengths of 496/523 nm ($\lambda_{exc}/\lambda_{em}$), under weak agitation. At t = 30 s, lipoplexes (corresponding to 100 nM DNA final concentration) were added in the cuvette, and the accessible DNA increased the fluorescence of the SYBR probe. At t = 100 s, 10 μL of Triton X100 10% (v/v) was added to disrupt the liposomes, allowing the total amount of DNA to be complexed by the SYBR probe. Final fluorescence was recorded at t = 200 s. The percentage of aptamer encapsulation was calculated using the Eq. (2), where the initial intensity is the average fluorescence intensity between time points 30 and 100 s and the final intensity is the average fluorescence intensity between time points 100 and 200 s.

$$\text{EE}\ (\%) = 100 - \left(\frac{\text{Initial intensity}}{\text{Final intensity}}\right) * 100\% \quad (2)$$

2.6. Stability of lipoplexes

Lipoplexes, containing Doxapt-30 at N/P = 3, were prepared in 5% dextrose and 5 mM NaCl and kept at 37 °C. Encapsulation efficiency of aptamers was measured by direct and indirect methods at 0, 4 and 24 h to quantify the release of the Doxapt-30 aptamer. A similar study was conducted on lipoplexes containing Apt-Ctrl-1 at N/P = 3. Encapsulation efficiency of aptamers was measured at 0, 1, 2, 6, 8, 12 and 24 h in PBS at 37 °C. Colloidal stability studies were conducted on another batch of lipoplexes containing Doxapt-30 at N/P = 3 diluted 3:1 in phosphate buffered saline (PBS) at pH 7.4. The hydrodynamic diameter and polydispersity index were measured at days 0, 3, 5 and 7.

2.7. Doxorubicin-loaded lipoplexes

Doxorubicin stock solutions were prepared in Tris/NaCl buffer (5 mM/145 mM, pH 7.4). Equal volumes of lipoplexes and doxorubicin solutions were combined at various doxorubicin/aptamer molar ratios (1:1–25:1). Noteworthy, Poly-Doxapt was composed of two pre-complexed strands and considered as one molecule in the calculations (124 nucleic acid for one DNA molecule). The mixture was incubated for 25 min, at 1000 rpm and 30 °C, and stored in the refrigerator in the dark before use. Samples were used immediately to determine their encapsulation efficiency. N/P ratio and drug/aptamer ratio were optimized for each formulation (Table 3). Optimized formulations of doxorubicin-loaded lipoplexes were used without purification for *in vitro* release and cytotoxicity studies, to ensure that doxorubicin total amount was identical in all samples.

As for Doxil-like liposomes, doxorubicin stock solution was added to pH-gradient liposomes (1:1 v/v) to obtain drug/lipid ratio of 0.1 and the mixture was incubated at 50 °C, for 25 min and 1000 rpm. No further purification method was applied for subsequent testing.

Doxorubicin encapsulation was determined indirectly by fluorescence assay. Doxorubicin-loaded lipoplexes were centrifuged 60 min at 18,500*g* at room temperature and supernatant was collected. Free doxorubicin was quantified by fluorescence using a Safire microplate reader (λ_{ex} 485 nm; λ_{em} 585 nm) against a calibration curve. Doxorubicin encapsulation efficiency was determined using Eq. (3). The final drug/lipid (D/L) ratio was determined using Eq. (4).

$$\text{EE}\ (\%) = \frac{(\text{Feeding doxorubicine}) - (\text{Free doxorubicin})}{(\text{Feeding doxorubicin})} * 100\% \quad (3)$$

$$\text{D/L}\ (\text{w/w}) = \frac{(\text{Feeding doxorubicin} - \text{Free doxorubicin})}{\text{Total lipid} + \text{Feeding doxorubicin}} \quad (4)$$

2.8. Release kinetics of doxorubicin-loaded lipoplexes

Each formulation of doxorubicin-loaded lipoplexes was prepared in quadruplicate and used without purification to ensure identical initial doxorubicin amounts in each condition. 1 mL of doxorubicin-loaded lipoplexes (13 μM of doxorubicin) was added to dialysis bags (6–8 kDa MWCO, Spectra/Por, Spectrum Laboratories, Inc.) and immerged into 100 mL of PBS pH 7.4 (n = 3) or acetate buffer pH 5 (n = 1). The whole set-up was moderately stirred at 37 °C and protected from light. 0.8 mL samples were withdrawn from the external medium at predetermined time points over 48 h and replaced by fresh medium. Samples were stored at 4 °C before analysis with a UPLC-Fluorescence against a calibration curve prepared from the initial doxorubicin solution. Briefly, the UPLC system (Shimadzu-Prominence UFLC, Shimadzu USA Manufacturing Inc. Mandel) consisted of a LC-20AD binary pump, a DGU-20A5 solvent degasser, a SIL-20AC HT refrigerated, a CT0-20AC column oven and a RF-20AXS fluorescence detector. Mobile phase A: water/0.1% formic acid. Mobile phase B: acetonitrile. Flow rate: 0.7 mL/min. Gradient A decreased linearly from 90 to 60% between 0.25 and 5.5 min; followed by recovery of 90% A in 0.2 min, then equilibration for 4.5 min at 90% A. Total run time: 9 min. Injection volume: 50 μL. The column (Poroshell 120 EC-C18, 3.0 × 30 mm, 2.7 μm equipped with a pre-column Agilent EC-C18, 3.0 × 5 mm, 2.7 μm) was kept at 30 °C and retention time of doxorubicin was of 5.4 min. Detection of doxorubicin was measured at λ_{exc} = 485 nm/λ_{em} = 585 nm. The kinetics curves were also fitted using a double exponential function and the amplitude and rate constants for drug release and drug degradation were obtained from the best fit.

2.9. Cell viability assay

HeLa cells were initially cultured in Eagle's Minimum Essential Medium (EMEM, ATCC® 30-2003™) supplemented with 10% fetal bovine serum (FBS) and 100 units/mL Penicillin-streptomycin (Life Technologies, Burlington, ON). Cells were incubated at 37 °C with 5% CO_2. Cells were seeded in a 96-well plate at a density of 5×10^3 cells per well. After 24 h, fresh culture medium and optimized formulation were added to each well, with final concentrations of doxorubicin ranging from 0.01 to 25 μM per well. In each plate, the blank formulation (without doxorubicin) was tested for its cytotoxicity at its highest concentration used. After 48 h incubation, the cells were rinsed with DPBS 1×. Resazurin in EMEM (final concentration of 44 μM in each well) was added. The cells were incubated an additional 3 h. Absorbance was measured at 570 nm and 600 nm to determine the metabolic reduction of resazurin. IC_{50} was determined using GraphPad Prism 6 and a normalized dose-response inhibition curve fitting. Each curve was made in triplicate or more.

2.10. Tobramycin-loaded lipoplexes

Tobramycin sulphate was fluorescently labeled by Cy5. Synthesis details and characterization are described in supplementary information. The binding affinity of Apt-Ctrl-1 for Tobramycin-Cy5 was measured by fluorescence assay as described in supplementary information.

Before liposome preparation, Ctrl-Apt-1 was denatured 5 min at 95 °C, vortexed for 1 min and annealed at room temperature. Aptamer

and Tobramycin-Cy5 were first mixed in equal volumes at increasing molar ratios (0.5, 1, 2, 3, 5 tobramycin/aptamer) in 5% dextrose and 5 mM NaCl. Liposomes (DOTAP/Chol/DSPE-PEG$_{2000}$ 50/48/2 molar ratio) were previously prepared in 5% dextrose and 5 mM NaCl as described in Section 2.3. They were mixed at equal volume (N/P = 3) with the tobramycin/aptamer solutions or tobramycin solutions without Apt-Ctrl-1 (negative control). The lipoplexes were incubated for 25 min at 30 °C at 1000 rpm before being centrifuged 60 min at 18,500*g* at room temperature. Free Tobramycin-Cy5 was quantified in the supernatant by fluorescence using a Safire microplate reader (λ_{exc} 649 nm; λ_{em} 670 nm) against a calibration curve. Tobramycin encapsulation efficiency and the final drug/lipid (D/L) ratio were determined using Eqs. (3) and (4) adapted to tobramycin. Experiment was run in triplicate.

2.11. Statistical analysis

Statistical analysis was carried out using PRISM 6.01 software (GraphPad, CA, USA). For zeta potential measurements, statistical analysis was performed with two-tailed Student's *t*-test: *$p < 0.05$; **$p < 0.01$; ***$p < 0.001$. To determine statistically significant encapsulation efficiency differences, a two-way ANOVA analysis was performed. To determine statistically significant IC_{50} differences, a one-way ANOVA analysis was performed. In both cases, p values for multiple comparisons were adjusted using the Bonferroni correction. A p value of ≤0.05 was considered significant.

3. Results

3.1. Aptamer design and affinity for doxorubicin

In this study, we used aptamers as the driving force to actively load a drug into the liposomes. Doxorubicin was selected as a model drug for several reasons. First, it represents a good example of successful active drug loading via ammonium sulphate gradient into liposomes [22]. Second, a doxorubicin-binding DNA aptamer has already been reported and validated in the literature [33,36]. Third, binding of doxorubicin to aptamers can be easily monitored by fluorescence measurements, which makes it a suitable model drug candidate for formulation optimization [37]. We hypothesized that tuning the affinity of the aptamers should impact the loading and the release rate of the drug from liposomes, therefore we designed a series of aptamer sequences with various binding properties (Fig. 1A, Table S1). All the aptamers include the doxorubicin specific sequence, designed as Doxapt-28 [36]. Doxapt-30 possesses an extra base pair that should stabilize the double strand section and increase the affinity of the aptamer for its ligand [33]. Coop-Doxapt, a two-binding-site aptamer reported by Simon et al., contains two binding sites and displays a cooperative binding behaviour [33]. Inspired by polymer-like aptamers [38], we also created Poly-Doxapt to improve aptamer packing into the liposome. Finally, two sequences were used as negative controls: Apta-Ctrl-1 is a 21-nucleotide aptamer designed for tobramycin, which presents a hairpin structure, but no specificity for doxorubicin [39] and Apta-Ctrl-2 is a 30mer of poly-

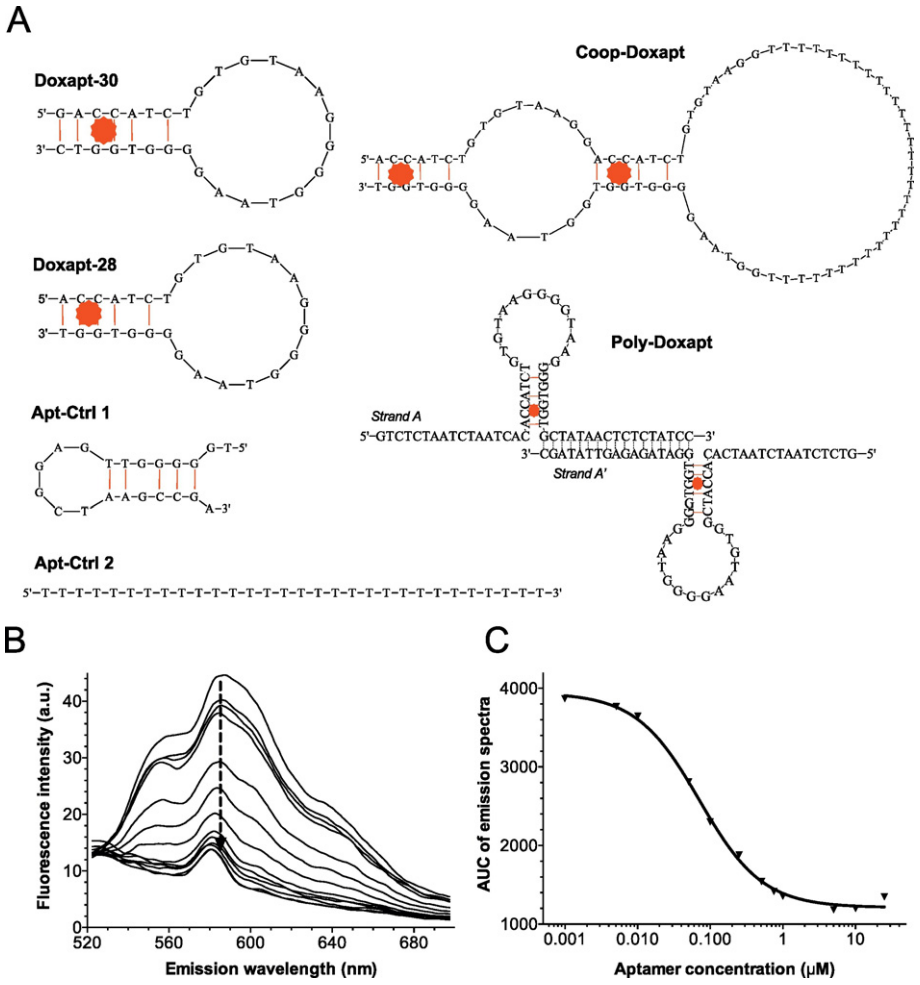

Fig. 1. Design of doxorubicin-binding aptamers with various affinities. A) Structure of DNA sequences designed for doxorubicin. The binding site for doxorubicin is suggested by a dot. B) Smoothed emission spectra of doxorubicin (100 nM in 5% dextrose and 5 mM NaCl) with increasing concentration of Poly-Doxapt (from top to bottom, 0, 0.001, 0.005, 0.01, 0.05, 0.1, 0.25, 0.75, 1, 5, 10, 25 μM). C) Representative determination of affinity binding constant K_D for Poly-Doxapt. Each point represents the area under the curve of the fluorescence emission spectra showed in B).

Table 1
Characteristics of aptamers used in this study and their affinity constants (K_D) for doxorubicin.

Formulation	Doxapt-28	Doxapt-30	Coop-Doxapt	Poly-Doxapt	Apt-Ctrl-1	Apt-Ctrl-2
Nucleotides	28	30	86	62 + 62	21	30
Binding sites	1	1	2	2	0	0
K_D (nM)[a]	380 ± 45	334 ± 29	160 ± 36	68 ± 6	>1000	ND[b]

[a] Determined by fluorescence assay, as shown in Figs. 1, S1–S5.
[b] Fluorescence of doxorubicin was not quenched sufficiently to determine a dissociation constant (see Fig. S5).

thymine without any secondary structure. Following the proof-of-concept demonstration, the strategy was applied to another drug, tobramycin, using the reported specific aptamer sequence Apt-Ctrl-1 (Fig. 1A) [39].

Once intercalated into a DNA, doxorubicin fluorescence is quenched, which allows monitoring of its interaction with different aptamer structures (Fig. 1B) [37]. Dissociation constants (K_D) of the various aptamers in the medium used for liposomal formulation (dextrose 5%, 5 mM NaCl) can thus be obtained by fitting the fluorescence intensity of doxorubicin to increasing concentrations of aptamers. A representative example of such curves is displayed in Fig. 1C (see also Figs. S1–S5) and the summary of all K_D is provided in Table 1. Doxapt-28 (380 nM) and Doxapt-30 (334 nM) exhibit K_D values in agreement with previous reports, despite variation of the medium (Table 1) [33]. Both Coop-Doxapt and Poly-Doxapt exhibited a higher affinity for doxorubicin (160 ± 36 nM and 68 ± 6 nM respectively), confirming the relevance of multivalent aptamers. However, under the liposomal formulation conditions, Coop-Doxapt did not display a higher cooperativity for doxorubicin binding as this has been previously observed at higher temperature (30 °C) and ionic strength (50 mM) (Fig. S3) [33]. This is likely due to the fact that the cooperativity level of DNA recognition elements is highly dependent on temperature and ionic strength variations [40]. Finally, Apt-Ctrl-1 displayed reduced affinity for doxorubicin (K_D > 1000 nM) while Apt-Ctrl-2 did not quench the fluorescence at an appreciable amount to determine a dissociation constant. Overall, this collection of aptamers exhibits dissociation constants for doxorubicin ranging from 68 nM to >1000 nM.

3.2. Lipoplex preparation and characterization

Aptamers were incorporated into cationic liposomes *via* electrostatic interactions. The liposome composition (DOTAP/Chol/DSPE-PEG_{2000} 50/48/2) was inspired by the widely reported lipid formulations used in gene delivery [41]. Similarly to these latter systems, the physicochemical properties of lipoplexes rely on the charge ratio N/P (amino group of DOTAP *vs.* phosphate group of nucleotide). As illustrated by Doxapt-30 lipoplexes, the liposome increased in size upon incubation with aptamers and exhibited aggregation at the charge ratio N/P = 2, as witnessed by the higher diameter and polydispersity index (Fig. 2A). Colloidal stability is recovered with an excess of cationic charges (N/P ≥ 3), resulting in lipoplexes smaller than 200 nm diameter, with low polydispersity and positive ζ potential (Fig. 2A & B). Similar behaviour was confirmed for all aptamers (Fig. S6). Aptamer complexation efficiency, quantified by the remaining DNA in solution, was also improved with increasing charge ratios. Aptamers presenting one binding site (Doxapt-28 and Doxapt-30) required N/P = 3 to be fully encapsulated into liposomes, whereas N/P = 2 was sufficient for Coop-Doxapt and Poly-Doxapt to achieve complete DNA complexation (Fig. 2C). These results were confirmed by directly measuring the concentration of aptamers within lipoplexes (Table S2). Except for Coop-Doxapt and Poly-Doxapt, the values obtained (≥94% for all aptamers) demonstrated that DNA was mainly encapsulated within lipoplexes; only a minor quantity was adsorbed on the surface. Noteworthy, ζ potential of Poly-Doxapt and Coop-Doxapt were still negative at N/P = 2, suggesting the presence of DNA strains adsorbed on the surface of the lipoplexes

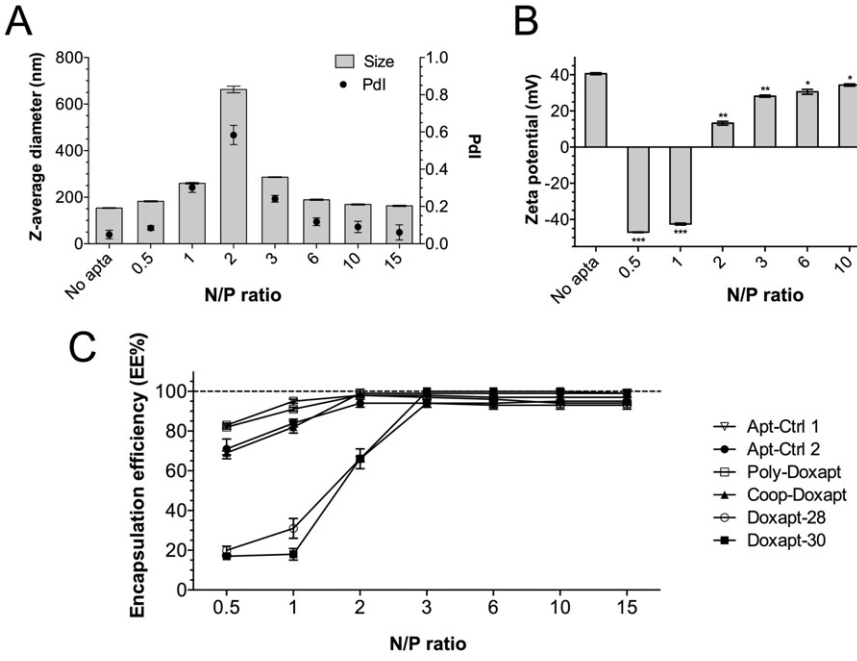

Fig. 2. Optimization of aptamer-loaded liposomes (DOTAP/Chol/DSPE-PEG_{2000} 50/48/2 molar ratio) according to the N/P ratio (amine of DOTAP/phosphate of nucleobases). A) Hydrodynamic diameter (size) and polydispersity index (PdI) and B) zeta potential measurements of lipoplexes encapsulating Doxapt-30. Statistical analysis performed with two-tailed Student's *t*-test: *p < 0.05; **p < 0.01; ***p < 0.001. C) Encapsulation efficiency of all aptamers within cationic lipoplexes. Results are reported as the mean value of 3 measurements, ± standard deviation of the mean.

Table 2
Stability of encapsulated aptamers over 24 h at 37 °C in dextrose 5% NaCl 5 mM. Liposomes DOTAP/Chol/DSPE-PEG$_{2000}$ 50/48/2 encapsulating Doxapt-30 (ratio N/P = 3) were assayed for their content in aptamers using the direct and indirect method. Results are reported as the mean value of 3 experiments, ± standard deviation of the mean.

	Time (h)		
	0	4	24
Direct method	98.3 ± 0.1%	98.1 ± 0.1%	98.2 ± 0.1%
Indirect method	98.6 ± 0.6%	99.1 ± 0.3%	97.0 ± 1.2%

(Table 3). This could be due to the longer sequence of nucleotides of Coop-Doxapt and Poly-Doxapt (86 and 124 nucleotides, respectively) as compared to other aptamers (28–30 nucleotides). Adsorption of Coop-Doxapt was confirmed since only 46% of the aptamer was actually encapsulated within the lipoplex structure, as determined by direct measurement (Table S2). As for Poly-Doxapt, direct and indirect methods corroborate that >83% of aptamers were encapsulated within liposomes (Table S2). This result suggests that, despite the negative zeta potential, aptamers were tightly bound to the lipoplex structure and were not accessible to the fluorescent dye.

In addition, the aptamers remained encapsulated for at least 24 h at 37 °C, for Doxapt-30 (Table 2) as well as for the control sequence Apt-Ctrl-1 (Table S3). For each aptamer, optimal N/P ratio was selected as the lowest ratio leading to stable lipoplexes and maximal encapsulation of aptamer (Table 3). Final lipoplexes exhibited diameters ranging from 170 to 290 nm with low polydispersity indexes, and almost complete complexation of aptamers. Lipoplexes exhibited good colloidal stability for 7 days in PBS at 37 °C (Fig. S7).

3.3. Encapsulation of doxorubicin

Aptamer-loaded lipoplexes were further incubated with doxorubicin at increasing doxorubicin/aptamer molar ratios, and doxorubicin encapsulation was quantified by fluorescence of free drug after centrifugation. A representative behaviour is reported in Fig. 3A with Doxapt-30. Encapsulation efficiency (EE) reached ≥85% doxorubicin for up to 2 drug molecules per aptamer, close to the efficiency of the sulphate gradient method of Doxil-like liposomes (Fig. 3A). The active role of aptamers in the loading capacity was confirmed by a series of controls. Passive encapsulation was estimated to range from 5 to 25% using cationic or plain liposomes, respectively (Fig. 3A). Moreover, Apt-Ctrl-2 (poly-thymine) was not able to drag doxorubicin into the liposomes whereas Apt-Ctrl-1, presenting a hairpin structure, displayed 45% reduction compared to the highest doxorubicin encapsulation value, which confirmed the higher specificity of Doxapt-30 for doxorubicin. Interestingly, the lipoplexes of Doxapt-30 enabled the loading of >2 doxorubicin molecules per aptamer, although this sequence is designed to have only one binding site. Above this doxorubicin/aptamer ratio, additional drug loading was reduced, leading to a decrease of EE %. Nonetheless, the final drug/lipid ratio (D/L) still increased up to 20 doxorubicin/aptamer (Fig. 3A). Similar trends were also observed for Coop-Doxapt and Poly-Doxapt, which were found to load up to 8 and 15 equivalents of doxorubicin with >80% EE for Coop-Doxapt and Poly-Doxapt, respectively (Fig. 3B). Therefore, the adsorption of Coop-Doxapt on the surface of lipoplexes did not seem to impact its loading capacity. In contrast, Doxapt-28 loaded lipoplexes were not able to encapsulate >45% doxorubicin. This could be due to the deletion of one base pair in the Doxapt-28 sequence (Fig. 1A), which leads to a less stable stem-loop (1 GC less, around 2 kcal/mol) [42]. The Doxapt-28 stem-loop may be destabilized in the lipoplex structure, which would impair doxorubicin binding. Therefore, Doxapt-28 appears as a negative control of Doxapt-30, exhibiting the closest sequence as possible with significantly different loading properties. A summary of the optimized formulations is presented in Table 3. For each aptamer, we selected the formulation exhibiting high encapsulation of both aptamer and doxorubicin, with a minimum amount of excipients. Furthermore, the addition of doxorubicin to lipoplexes did not significantly affect neither the size nor the polydispersity of the formulations (Table 3). Further studies were conducted using twice the doxorubicin amount as compared to the number of binding sites, to maximize drug loading for both single and double-binding sites aptamers.

3.4. Release kinetics of doxorubicin-loaded lipoplexes

Aptamers improve the loading capacity of liposomes but do their presence impact drug release rate? To test this question, we measured the release kinetics of doxorubicin from the aptamer-loaded lipoplexes by employing a dialysis method (Fig. 4). Lipoplexes were prepared at optimal ratios and were not purified before dialysis, to ensure similar initial doxorubicin concentration. Kinetics display a bi-exponential profile with the fastest transition representing the release of doxorubicin from the lipoplexes and the slowest transition the elimination of doxorubicin over time (Table 4 and Fig. S8). The elimination of doxorubicin concentration after several hours (Fig. 4) might be due to the degradation of doxorubicin at pH 7.4 at 37 °C and its adsorption to surfaces

Table 3
Summary of the characteristics for the optimized formulations of liposomes, lipoplexes containing aptamers and doxorubicin-loaded lipoplexes. All liposomes were cationic liposomes (DOTAP/Chol/DSPE-PEG$_{2000}$ 50/48/2 molar ratio) except for Doxil-like (DSPC/Chol/DSPE-PEG$_{2000}$ 55/40/5 molar ratio). Results are reported as the mean value of 3 measurements, ± standard deviation of the mean.

Formulation		Doxapt-28	Doxapt-30	Coop-Doxapt	Poly-Doxapt	No apta	Doxil-like	Apt-Ctrl-1	Apt-Ctrl-2
Liposomes	Z-average diameter (nm)	139 ± 3	154 ± 2	139 ± 3	139 ± 3	139 ± 3	187 ± 6	139 ± 3	139 ± 3
	PdI	0.082 ± 0.001	0.049 ± 0.012	0.082 ± 0.001	0.082 ± 0.001	0.082 ± 0.001	0.038 ± 0.036	0.082 ± 0.001	0.082 ± 0.001
Aptamer-loaded lipoplexes	Z-average diameter (nm)	171 ± 3	286 ± 2	230 ± 3	283 ± 7	139 ± 3	187 ± 6	242 ± 5	206 ± 4
	PdI	0.058 ± 0.018	0.241 ± 0.018	0.058 ± 0.019	0.222 ± 0.023	0.082 ± 0.001	0.038 ± 0.036	0.069 ± 0.013	0.048 ± 0.033
	Zeta potential (mV)	22.4 ± 1.2	28.2 ± 0.6	−19.4 ± 0.6	−24.7 ± 0.6	24.9 ± 0.6	−4.8 ± 1.1	4.53 ± 0.6	17.6 ± 1.6
	Ratio N/P	3	3	2	2	N/A	N/A	3	3
	EE% aptamers[a]	94 ± 2%	100 ± 0%	99 ± 2%	98 ± 1%	N/A	N/A	94 ± 1%	99 ± 0%
Doxorubicin and aptamer-loaded lipoplexes	Z-average diameter (nm)	197 ± 2	236 ± 6	254 ± 2	312 ± 4	154 ± 2	181 ± 3	285 ± 5	204 ± 2
	PdI	0.058 ± 0.018	0.047 ± 0.048	0.062 ± 0.002	0.172 ± 0.007	0.074 ± 0.008	0.063 ± 0.010	0.075 ± 0.011	0.068 ± 0.029
	Zeta potential (mV)	16.3 ± 0.8	15.9 ± 0.7	−28.1 ± 1.7	−28.8 ± 1.2	20.9 ± 0.9	−11.5 ± 0.1	8.81 ± 0.7	5.7 ± 0.5
	Ratio Dox/Apta	2	2	4	4	N/A	N/A	2	2
	EE% Dox[b]	28 ± 7%	84 ± 2%	73 ± 3%	86 ± 1%	5 ± 3%	98 ± 1%	39 ± 0%	7 ± 5%
	Final D/L ratio[c]	0.0034	0.0092	0.0088	0.0069	0.0006	0.098	0.0062	0.0008

[a] Determined by indirect method using Eq. (1).
[b] Determined by indirect method using Eq. (3).
[c] D/L: Drug/Lipid ratio (w/w) determined using Eq. (4).

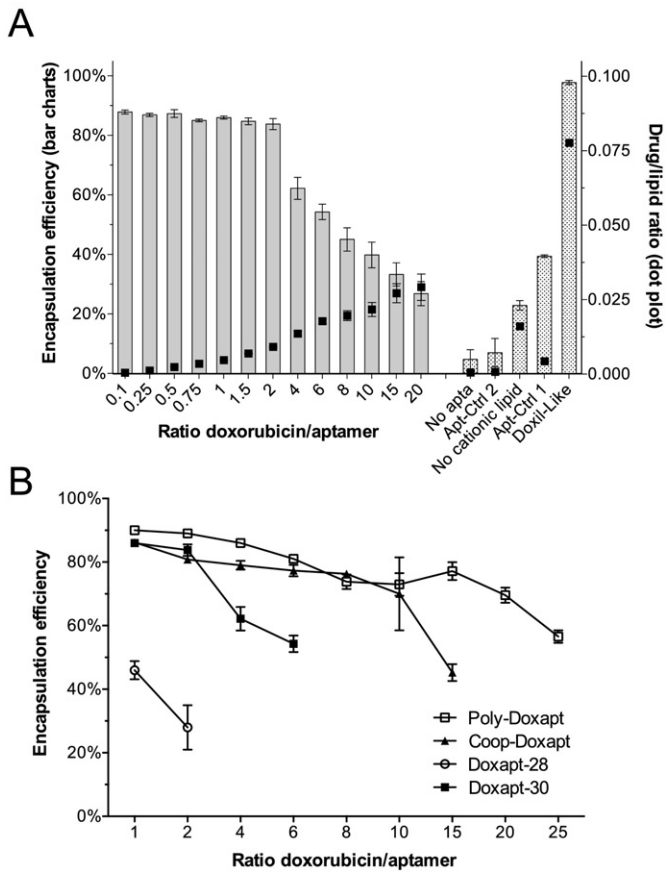

Fig. 3. Optimization of doxorubicin loading into aptamer-loaded lipoplexes. A) Doxorubicin encapsulation efficiency (%, bar charts, left) and final drug/lipid (D/L) ratio (w/w, dot plot, right) of Doxapt-30 lipoplexes (N/P = 3) at increasing molar ratios of doxorubicin/aptamer. 'No apta' control consisted of the cationic liposome (DOTAP/Chol/DSPE-PEG_{2000} 50/48/2 molar ratio) without any DNA. Apt-Ctrl-1 and Apt-Ctrl-2 were assessed at N/P = 3 and doxorubicin/aptamer = 2. 'No cationic lipid' is a liposome of POPC/cholesterol/DSPE-PEG_{2000} 55/40/5 representative of a neutral formulation for passive encapsulation, tested at D/L = 0.086. Doxil-like liposome was assessed at a D/L = 0.1. B) Encapsulation efficiency of doxorubicin within all aptamer-loaded lipoplexes. For each aptamer, N/P ratio was selected according to the optimized formulation (Table 3): N/P = 2 for Poly-Doxapt and Coop-Doxapt. N/P = 3 for Doxapt-28 and Doxapt-30. Results are reported as the mean value of 3 experiments, ±standard deviation of the mean.

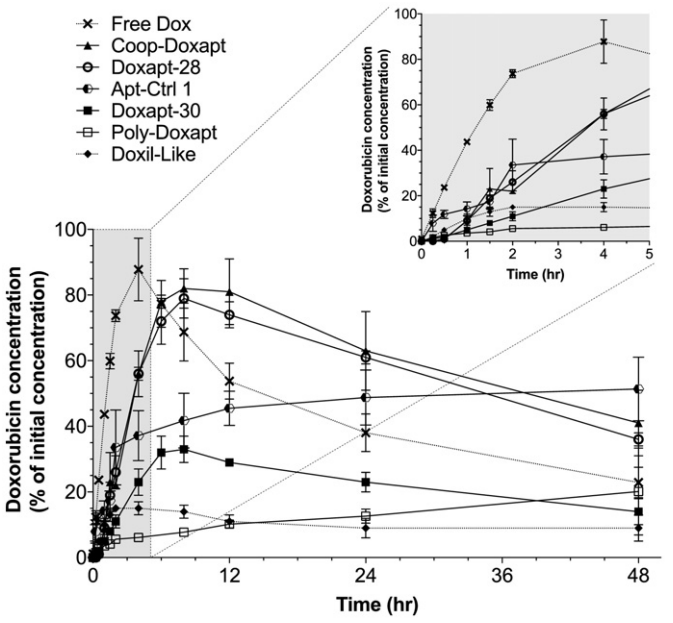

Fig. 4. Release of doxorubicin at 37 °C in PBS (pH 7.4) from optimized formulations of doxorubicin-loaded lipoplexes (see Table 3). 'Free Dox' corresponds to the initial amount of doxorubicin (1 mL of 15 μM doxorubicin) placed in the dialysis bag. Results are reported as the mean value of 3 experiments, ±standard deviation of the mean.

(dialysis bags as well as sampling vials), as previously described [43,44]. In agreement with literature, Doxil-like liposomes exhibited a lower release efficiency (<15% after 48 h, Fig. 4) [22,45] but the observed release rate was found similar to the rate obtained for free doxorubicin control (Table 4). This could be due to some doxorubicin adsorbed on the liposome surface, which was washed out in the first hour. Interestingly, quite different profiles were obtained for the series of lipoplexes. The high-loading Coop-Doxapt lipoplexes, for example, released 5-fold more doxorubicin than the Doxil-like liposomes at a 5-fold slower rate ($0.20 \pm 0.05\ h^{-1}$) reaching 80% of drug release after 10 h (Fig. 4). This suggests that doxorubicin release was slowed down by the binding to the aptamer but the adsorption of Coop-Doxapt on the lipoplex surface favored doxorubicin extensive release. Poly-Doxapt, which possesses the highest affinity for doxorubicin, released doxorubicin 5-fold slower than the Coop-Doxapt ($0.04 \pm 0.01\ h^{-1}$), which resulted in only 20% of doxorubicin being released after 48 h, similar to the Doxil-like formulation (Fig. 4). Doxapt-30, which has an intermediate affinity (K_D = 334 nM), displayed a sustained release, achieving 30% of release after 12 h with a release rate similar to Coop-Doxapt ($0.23 \pm 0.06\ h^{-1}$). Doxapt-28 also displayed a similar release rate (Table 4), despite its low drug loading efficiency, while Apta-Ctrl 1 displayed a significantly faster release rate of $0.38 \pm 0.07\ h^{-1}$, in agreement with its lower affinity for doxorubicin. Both latter formulations released more doxorubicin than Doxapt-30 (75% and 45% of initial doxorubicin after 12 h, respectively), probably due to the residual unencapsulated doxorubicin. As a control, we demonstrated that no leakage of Doxapt-30 nor the Apta-Ctrl-1 was detected over a 24 h period in the same conditions, showing no sequence specific effect on aptamer release (Tables 2 & S3). We also investigated the behaviour of doxorubicin loaded lipoplexes at acidic pH, to mimic the endosomal conditions. Interestingly, the relative behaviour of aptamers was maintained albeit the acidic conditions decreased doxorubicin elimination, in agreement with literature [44], which slightly increased the extent of drug release (Figs. S9 and S10). Coop-Doxapt and Doxapt-30 still exhibited similar release rates (0.30 and $0.28\ h^{-1}$, respectively, Table 4). Here again, Coop-Doxapt released over 90% of its drug in 12 h (Fig. S9) whereas Doxapt-30 sustained its release (53% doxorubicin released in 12 h). The higher affinity of Poly-Doxapt severely reduced doxorubicin release (22% in 12 h, Fig. S9) as well as the release rate ($0.078\ h^{-1}$, Table 4). The negative controls, Doxapt-28 and Apta-Ctrl-1, still quickly released 82 and 72% of their content after 12 h, respectively (Fig. S9). Overall, these results suggest that aptamers slowed down the release of drug according to their specific affinity, which allows to control drug diffusion and release from lipoplexes.

3.5. Cell viability assay

Modifying the release kinetics of a drug has a direct impact on its therapeutic efficacy. To explore this impact, we completed our study by assessing the cytotoxic activity of doxorubicin in the optimized formulations on HeLa cells (Fig. 5A). Free doxorubicin presented an IC_{50} of 1.5 ± 0.6 μM, in agreement with the literature [46]. Doxil-like formulation exhibited significantly higher values of IC_{50}, up to 38 μM, reflecting of the low immediate bioavailability of doxorubicin from these liposomes. Doxapt-30 improved 4 times the therapeutic efficacy of Doxil-like formulation, exhibiting similar cytotoxicity as free doxorubicin, notwithstanding its sustained release. Coop-Doxapt and Apta-Ctrl 1 also exhibited similar cytotoxicity to free doxorubicin, probably due to their extensive drug release over 48 h. Conversely, Poly-Doxapt exhibited similar cytotoxicity to Doxil-like formulations, in agreement with its

Table 4
Kinetic parameters of doxorubicin release from the aptamer-loaded lipoplexes at pH 7.4 (see Fig. 4) and pH 5 (see Fig. S9). All kinetics were fitted using a bi-exponential fit. The fastest transition (described by Amplitude 1 and Rate 1) represents the release of doxorubicin from the lipoplexes and the slowest transition (described by Amplitude 2 and Rate 2) the degradation of doxorubicin over time. No degradation was evidenced at pH 5.

		Free Dox	Doxil-like	Coop-Doxapt	Poly-Doxapt	Doxapt-30	Doxapt-28	Apta-Ctr-1
pH 7.4	Amp 1[a]	−102 ± 8	−16 ± 2	−136 ± 23	−21 ± 4	−52 ± 9	−130 ± 20	48 ± 2
	Rate 1[b]	0.8 ± 0.1	1.2 ± 0.3	0.20 ± 0.05	0.04 ± 0.01	0.23 ± 0.06	0.20 ± 0.04	0.38 ± 0.07
	Amp 2[a]	99 ± 8	16 ± 1	128 ± 25	–	49 ± 10	123 ± 21	–
	Rate 2[b]	0.039 ± 0.006	0.016 ± 0.005	0.025 ± 0.007	–	0.028 ± 0.007	0.027 ± 0.007	–
pH 5	Amp 1[a]	–	–	−93 ± 2	−34 ± 1	−55 ± 2	−80 ± 5	73 ± 3
	Rate 1[b]	–	–	0.30 ± 0.01	0.078 ± 0.007	0.28 ± 0.03	0.52 ± 0.07	0.30 ± 0.06

[a] In %.
[b] h^{-1}.

low doxorubicin release, in addition to its negative zeta potential and low N/P ratio, which may reduce cellular uptake [47]. As a control of lipoplex influence, the cell viability was determined after incubation with the highest concentration of aptamer-loaded lipoplexes without doxorubicin (Fig. 5B). The four blank lipoplexes formulations exhibited no toxicity on HeLa cells at their highest concentration, and were better tolerated than Doxil-like formulation. Overall, these results demonstrate that aptamer binding to doxorubicin did not prevent therapeutic efficacy of the drug, and an adequate sequence design could even improve its availability as compared to ammonium sulphate gradient liposomes.

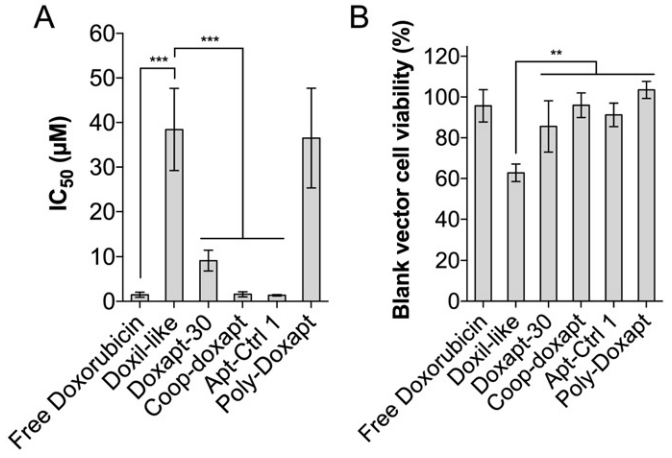

Fig. 5. Cytotoxic activity of doxorubicin in optimized formulations (see Table 3) on HeLa cells. A) IC_{50} values of doxorubicin in optimized formulations after 48 h. B) Cell viability of aptamer-loaded lipoplexes without doxorubicin at their highest concentration used for IC_{50} assay (corresponding to 25 μM doxorubicin). Results are reported as the mean value of 3 experiments, ±standard deviation of the mean. ***$p \leq 0.05$.

3.6. Application to tobramycin

Encouraged by this proof-of-concept, we further applied the strategy of aptamer-loaded lipoplexes to another drug, tobramycin. In the treatment of lung infection, liposomal tobramycin demonstrated drug retention in the lung and improved *in vivo* efficacy against bacterial infection as compared to the free drug [48]. Liposomes have also allowed a better accumulation close to the bacterial biofilm but the antibiotic activity was limited due to the low encapsulation efficiency of liposomes [49]. Indeed, tobramycin aminoglycoside structure is highly hydrophilic, which prevents its efficient encapsulation within liposomes. Therefore, this drug would significantly benefit from an active loading strategy using drug specific aptamers. Apt-Ctrl-1 was selected for its reported affinity for tobramycin [39]. To facilitate detection, tobramycin sulphate was labeled by fluorescent Cy5 (see synthesis and characterization in Supporting information). Binding affinity of Apt-Ctrl-1 for tobramycin was determined to be 1.15 ± 0.24 μM, slightly higher than doxorubicin-binding aptamers (Fig. 6A). Encapsulation of tobramycin in cationic liposomes was compared with or without aptamers (Fig. 6B). Interestingly, aptamers do also improve the encapsulation of tobramycin, reaching 5.8 times greater EE at high concentrations of tobramycin (45% against 8%, with and without aptamer, respectively) as well as drug/lipid ratio. These results demonstrate that an aptamer-loading strategy could successfully be used to improve the loading efficiency of various drugs into liposomes, especially for drugs with low encapsulation properties.

4. Discussion

Loading of drugs into liposomes is a critical step of the liposomal formulation, since it determines the amount of excipient required, as well as the factors governing the release rate of the drug [21]. In the passive loading method, the drug dissolved in the aqueous phase equilibrates with the liposome's internal medium, which limits its encapsulation efficiency. Higher scores can be achieved using a gradient method, such as

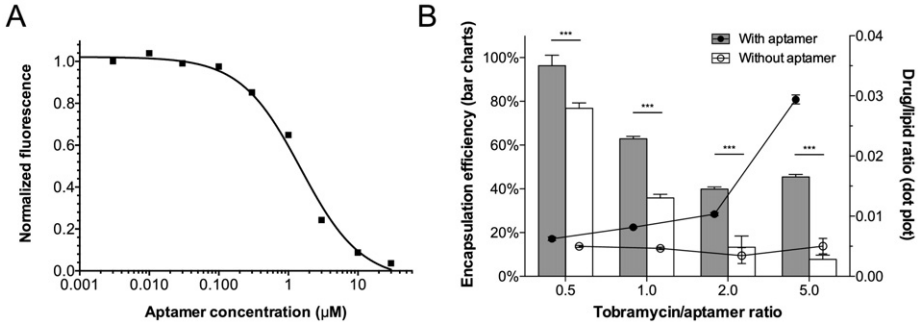

Fig. 6. Tobramycin encapsulation using aptamers. A) Binding affinity of Apt-Ctrl-1 for Tobramycin-Cy5. $K_D = 1.15 \pm 24$ μM. B) Tobramycin encapsulation efficiency (%, bar charts, left) and final drug/lipid ratio (w/w, dot plot, right) of aptamer-loaded lipoplexes (DOTAP/Chol/DSPE-PEG_{2000} 50/48/2 molar ratio, aptamer Ctrl-1, N/P = 3). Results are reported as the mean value of 3 experiments, ±standard deviation of the mean. ***$p \leq 0.05$.

pH or ions (ammonium sulphate, hydrogenophosphate, or metallic ion such as copper or manganese salts) [19]. In this strategy, the drug, when present inside the vesicle core, is converted to an ionic/salt form, which is unable to diffuse back through the lipid membrane, thus is retained into the liposome core. Unfortunately, this strategy also strongly impairs the release rate of the drug, and often requires an additional trigger [24]. This is confirmed by our results of Doxil-like formulation, which exhibited limited release (Fig. 4), high IC_{50} on HeLa cells, and even a non-negligible toxicity of the liposomes itself (Fig. 5).

We prepared liposomes with drug-specific aptamers to improve the loading capacity of liposomes. We selected aptamer technology because (i) their affinity can be tuned by controlling their nucleotide sequence or length [42], allowing to optimize the aptamer sequence according to the desired release properties; (ii) the binding does not change the protonation of the drug, therefore maintaining its diffusion and release ability [34] and (iii) aptamers could be designed for almost any target, suggesting this strategy could be applied to a large range of molecules [3].

The series of aptamers was designed to study the relationship between the sequence and the properties of aptamer-loaded lipoplexes. As expected, the affinity of aptamers varied according to their sequences and binding sites (Table 1). The results confirmed the specificity of the aptamer sequences for its drug since the binding is higher than the natural affinity of doxorubicin for random single or double-stranded DNA (Table 1) as well as aptamer/doxorubicin complexes reported in literature ($K_D \approx 600$ nM) [37]. However, Doxapt-28, presenting a similar affinity to Doxapt-30, was not able to encapsulate >50% of doxorubicin. Adding a base pair to the hairpin probably allowed a higher stabilization of the complex, which has already been reported [42]. The three other structures, although exhibiting different binding constants, demonstrated similar drug loading capacity (Table 3). This might be explained by the high concentration of the drug in the liposomal formulation (>10 times K_D) resulting in the saturation of aptamers. These conditions might also reveal secondary binding sites on aptamers, which results in the binding of >2 doxorubicin molecules per aptamer for Doxapt-30 and >8 and 15 molecules for Coop-Doxapt and Poly-Doxapt, respectively (Fig. 3). For the latter cases, the higher loading capacity may be linked to their longer sequence of nucleotides (86 and 124 nucleotides, respectively), revealing probably additional binding sites for doxorubicin. Interestingly, this behaviour was also observed for tobramycin (Fig. 6B), which was able to encapsulate up to 2.5 tobramycin equivalents, although designed with only one binding site. Although this non-specific binding was not detected in the binding affinity measurements (Fig. 1), it can be explained by the natural affinity of doxorubicin for nucleic acids or the electrostatic interactions of both cationic drugs with anionic nucleobases [37,50]. In addition, incorporation of DNA sequences into liposomes has been reported to strongly impact the structural organization of the liposome, resulting in densely packed lipoplexes, which might favor the retention of the drug [50,51]. Overall, aptamer incorporation into liposomes significantly improved their loading capacity, through specific as well as non-specific interactions with the drug.

Interestingly, our results show that release kinetics and therapeutic efficacy could be tuned according to the aptamer structure. We showed that drug binding to the aptamer slowed down the release rate of the drug in comparison to the free drug, according to its affinity constant. Doxapt-30 exhibited a slower release than Apt-Ctrl-1, which allowed a sustained release of the drug over 48 h. Nevertheless, a too high affinity might compromise the drug release from the lipoplex, as exemplified by Poly-Doxapt ($K_D = 68$ nM, <15% release in 48 h). Therefore, this latter system did not improve commercial formulation, as confirmed by the same therapeutic efficiency as Doxil-like (Fig. 5). Apart from the affinity, our results suggest that other sequence parameters impact the overall behaviour of the system. Coop-Doxapt, maybe due to its longer stem-loop, resulted in low encapsulation of aptamer within the lipoplex. The adsorption of ~50% Coop-Doxapt on the surface of liposomes still allowed doxorubicin complexation but favored its release in physiological conditions. Therefore, this system was not improved compared to free doxorubicin. In the other hand, the short Doxapt-28 sequence demonstrated that a minimal stability of the stem-loop is required to ensure drug binding ability within the lipoplex structure. In our study, Doxapt-30 exhibited the advantages of Doxil-like formulation without its limitations. Indeed, this sequence exhibits a specific affinity for doxorubicin and a high encapsulation efficiency within cationic lipoplexes, which resulted in a sustained release profile and an excellent therapeutic efficiency. In addition, this nucleotide sequence length limited the excipient mass required for doxorubicin loading, resulting in the highest drug/lipid ratio (Table 3).

5. Conclusion

In conclusion, we developed a new strategy of drug loading, by designing drug-specific aptamers to drive drugs into liposomes. Combining the advantages of aptamer specific properties and liposomal controlled release enable to achieve tunable properties according to the structure of the aptamer. We demonstrated the proof-of-concept using doxorubicin, but this strategy may be applied to a large variety of drugs, since aptamers can be synthetically prepared against about any target, from small molecules to whole cells. In particular, we showed that aptamers significantly improved the loading of hydrophilic tobramycin into liposomes. These results demonstrate the potential of aptamer technology for multifunctional drug delivery systems. In particular, adding drug specific sequences to a cancer-targeted aptamer could lead to better controlled drug delivery systems. Further improvements are currently focused on the drug/lipid ratio and the application to larger biomacromolecules.

Acknowledgements

Financial support from Reseau Québécois de Recherche sur le Médicament (RQRM), Hydro-Quebec and University of Montreal is acknowledged for the scholarship of K. Plourde. The authors want to thank Alexandre Melkoumov for synthesizing Tobramycin-Cy5 and performing statistical analysis, Warren Viricel for his help in graphics, Mihaela Friciu for her help in HPLC analysis and Jennifer Jean-Louis for the stability study. J. Leblond Chain thanks Pr N. Bertrand for insightful discussions.

Appendix A. Supplementary data

Supplementary data to this article can be found online at http://dx.doi.org/10.1016/j.jconrel.2017.02.026.

References

[1] A.D. Keefe, S. Pai, A. Ellington, Aptamers as therapeutics, Nat. Rev. Drug Discov. 9 (2010) 537–550.
[2] K.E. Maier, M. Levy, From selection hits to clinical leads: progress in aptamer discovery, Mol. Ther. Methods Clin. Dev. 5 (2016) 16014.
[3] G. Zhu, M. Ye, M.J. Donovan, E. Song, Z. Zhao, W. Tan, Nucleic acid aptamers: an emerging frontier in cancer therapy, Chem. Commun. 48 (2012) 10472–10480.
[4] K.-I. Matsunaga, M. Kimoto, C. Hanson, M. Sanford, H.A. Young, I. Hirao, Architecture of high-affinity unnatural-base DNA aptamers toward pharmaceutical applications, Sci. Report. 5 (2015) 18478.
[5] H. Sun, X. Zhu, P.Y. Lu, R.R. Rosato, W. Tan, Y. Zu, Oligonucleotide aptamers: new tools for targeted cancer therapy, Mol. Ther. Nucleic Acids 3 (2014) e182.
[6] P.R. Bouchard, R.M. Hutabarat, K.M. Thompson, Discovery and development of therapeutic aptamers, Annu. Rev. Pharmacol. Toxicol. 50 (2010) 237–257.
[7] Z. Liu, Y. Lu, Y. Pu, J. Liu, B. Liu, B. Yu, K. Chen, T. Fu, C.J. Yang, H. Liu, W. Tan, Using aptamers to elucidate esophageal cancer clinical samples, Sci. Report. 5 (2015) 18516.
[8] D. Oberthur, J. Achenbach, A. Gabdulkhakov, K. Buchner, C. Maasch, S. Falke, D. Rehders, S. Klussmann, C. Betzel, Crystal structure of a mirror-image L-RNA aptamer (Spiegelmer) in complex with the natural L-protein target CCL2, Nat. Commun. 6 (2015) 6923.
[9] Z. Zeng, C.-H. Tung, Y. Zu, A cancer cell-activatable aptamer-reporter system for one-step assay of circulating tumor cells, Mol. Ther. Nucleic Acids 3 (2014) e184.

[10] A. Shastri, L.M. McGregor, Y. Liu, V. Harris, H. Nan, M. Mujica, Y. Vasquez, A. Bhattacharya, Y. Ma, M. Aizenberg, O. Kuksenok, A.C. Balazs, J. Aizenberg, X. He, An aptamer-functionalized chemomechanically modulated biomolecule catch-and-release system, Nat. Chem. 7 (2015) 447–454.
[11] B.C. Wengerter, J.A. Katakowski, J.M. Rosenberg, C.G. Park, S.C. Almo, D. Palliser, M. Levy, Aptamer-targeted antigen delivery, Mol. Ther. 22 (2014) 1375–1387.
[12] B.S. Ferguson, D.A. Hoggarth, D. Maliniak, K. Ploense, R.J. White, N. Woodward, K. Hsieh, A.J. Bonham, M. Eisenstein, T.E. Kippin, K.W. Plaxco, H.T. Soh, Real-time, aptamer-based tracking of circulating therapeutic agents in living animals, Sci. Transl. Med. 5 (2013) (213ra165).
[13] H. Zhang, Y. Ma, Y. Xie, Y. An, Y. Huang, Z. Zhu, C.J. Yang, A controllable aptamer-based self-sssembled DNA dendrimer for high affinity targeting, bioimaging and drug delivery, Sci. Report. 5 (2015) 10099.
[14] O.C. Farokhzad, J. Cheng, B.A. Teply, I. Sherifi, S. Jon, P.W. Kantoff, J.P. Richie, R. Langer, Targeted nanoparticle-aptamer bioconjugates for cancer chemotherapy in vivo, Proc. Natl. Acad. Sci. U. S. A. 103 (2006) 6315–6320.
[15] Y.-H. Lao, K.K.L. Phua, K.W. Leong, Aptamer nanomedicine for cancer therapeutics: barriers and potential for translation, ACS Nano 9 (2015) 2235–2254.
[16] J. Liao, B. Liu, J. Liu, J. Zhang, K. Chen, H. Liu, Cell-specific aptamers and their conjugation with nanomaterials for targeted drug delivery, Exp. Op. Drug Deliv. 12 (2014) 493–506.
[17] K. Park, Facing the truth about nanotechnology in drug delivery, ACS Nano 7 (2013) 7442–7447.
[18] J.V. Natarajan, C. Nugraha, X.W. Ng, S. Venkatraman, Sustained-release from nanocarriers: a review, J. Control. Release 193 (2014) 122–138.
[19] J.O. Eloy, M. Claro de Souza, R. Petrilli, J.P. Barcellos, R.J. Lee, J.M. Marchetti, Liposomes as carriers of hydrophilic small molecule drugs: strategies to enhance encapsulation and delivery, Colloids Surf. B: Biointerfaces 123 (2014) 345–363.
[20] T.M. Allen, P.R. Cullis, Liposomal drug delivery systems: from concept to clinical applications, Adv. Drug Deliv. Rev. 65 (2013) 36–48.
[21] Y. Barenholz, Relevancy of drug loading to liposomal formulation therapeutic efficacy, J. Lipid Res. 13 (2003) 1–8.
[22] Y. Barenholz, Doxil® — the first FDA-approved nano-drug: lessons learned, J. Control. Release 160 (2012) 117–134.
[23] S. Bandak, D. Goren, A. Horowitz, D. Tzemach, A. Gabizon, Pharmacological studies of cisplatin encapsulated in long-circulating liposomes in mouse tumor models, Anti-Cancer Drugs 10 (1999) 911–920.
[24] E. Oude Blenke, E. Mastrobattista, R.M. Schiffelers, Strategies for triggered drug release from tumor targeted liposomes, Exp. Op. Drug Deliv. 10 (2013) 1399–1410.
[25] R. Mo, T. Jiang, R. DiSanto, W. Tai, Z. Gu, ATP-triggered anticancer drug delivery, Nat. Commun. 5 (2014).
[26] R. Mo, T. Jiang, Z. Gu, Enhanced anticancer efficacy by ATP-mediated liposomal drug delivery, Angew. Chem. Int. Ed. 53 (2014) 5815–5820.
[27] R. Mo, T. Jiang, W. Sun, Z. Gu, ATP-responsive DNA-graphene hybrid nanoaggregates for anticancer drug delivery, Biomaterials 50 (2015) 67–74.
[28] W.-C. Liao, C.-H. Lu, R. Hartmann, F. Wang, Y.S. Sohn, W.J. Parak, I. Willner, Adenosine triphosphate-triggered release of macromolecular and nanoparticle loads from aptamer/DNA-cross-linked microcapsules, ACS Nano 9 (2015) 9078–9086.
[29] M.R. Battig, B. Soontornworajit, Y. Wang, Programmable release of multiple protein drugs from aptamer-functionalized hydrogels via nucleic acid hybridization, J. Am. Chem. Soc. 134 (2012) 12410–12413.
[30] B. Soontornworajit, J. Zhou, M.P. Snipes, M.R. Battig, Y. Wang, Affinity hydrogels for controlled protein release using nucleic acid aptamers and complementary oligonucleotides, Biomaterials 32 (2011) 6839–6849.
[31] G. Zhu, J. Zheng, E. Song, M. Donovan, K. Zhang, C. Liu, W. Tan, Self-assembled, aptamer-tethered DNA nanotrains for targeted transport of molecular drugs in cancer theranostics, Proc. Natl. Acad. Sci. U. S. A. 110 (2013) 7998–8003.
[32] O. Boyacioglu, C.H. Stuart, G. Kulik, W.H. Gmeiner, Dimeric DNA aptamer complexes for high-capacity-targeted drug delivery using pH-sensitive covalent linkages, Mol. Ther. Nucleic Acids 2 (2013) e107.
[33] A.J. Simon, A. Vallée-Bélisle, F. Ricci, K.W. Plaxco, Intrinsic disorder as a generalizable strategy for the rational design of highly responsive, allosterically cooperative receptors, Proc. Natl. Acad. Sci. U. S. A. 111 (2014) 15048–15053.
[34] P. Sundaram, J. Wower, M.E. Byrne, A nanoscale drug delivery carrier using nucleic acid aptamers for extended release of therapeutic, Nanomed. Nanotechnol. Biol. Med. 8 (2012) 1143–1151.
[35] Z. Wu, L.-J. Tang, X.-B. Zhang, J.-H. Jiang, W. Tan, Aptamer-modified nanodrug delivery systems, ACS Nano 5 (2011) 7696–7699.
[36] A. Wochner, M. Menger, D. Orgel, B. Cech, M. Rimmele, V.A. Erdmann, J. Glökler, A DNA aptamer with high affinity and specificity for therapeutic anthracyclines, Anal. Biochem. 373 (2008) 34–42.
[37] V. Bagalkot, O.C. Farokhzad, R. Langer, S. Jon, An aptamer-doxorubicin physical conjugate as a novel targeted drug-delivery platform, Angew. Chem. Int. Ed. Eng. 45 (2006) 8149–8152.
[38] M.-G. Kim, J.Y. Park, W. Miao, J. Lee, Y.-K. Oh, Polyaptamer DNA nanothread-anchored, reduced graphene oxide nanosheets for targeted delivery, Biomaterials 48 (2015) 129–136.
[39] K.-M. Song, M. Cho, H. Jo, K. Min, S.H. Jeon, T. Kim, M.S. Han, J.K. Ku, C. Ban, Gold nanoparticle-based colorimetric detection of kanamycin using a DNA aptamer, Anal. Biochem. 415 (2011) 175–181.
[40] A.J. Simon, A. Vallée-Bélisle, F. Ricci, H.M. Watkins, K.W. Plaxco, Using the population-shift mechanism to rationally introduce "hill-type" cooperativity into a normally non-cooperative receptor, Angew. Chem. Int. Ed. 53 (2014) 9471–9475.
[41] H. Yin, R.L. Kanasty, A.A. Eltoukhy, A.J. Vegas, J.R. Dorkin, D.G. Anderson, Non-viral vectors for gene-based therapy, Nat. Rev. Genet. 15 (2014) 541–555.
[42] A. Porchetta, A. Vallée-Bélisle, K.W. Plaxco, F. Ricci, Using distal-site mutations and allosteric inhibition to tune, extend, and narrow the useful dynamic range of aptamer-based sensors, J. Am. Chem. Soc. 134 (2012) 20601–20604.
[43] M.J.H. Janssen, D.J.A. Crommelin, G. Storm, A. Hulshoff, Doxorubicin decomposition on storage. effect of pH, type of buffer and liposome encapsulation, Int. J. Pharm. 23 (1985) 1–11.
[44] D.C. Wu, C.M. Ofner, Adsorption and degradation of doxorubicin from aqueous solution in polypropylene containers, AAPS PharmSciTech 14 (2013) 74–77.
[45] L. Silverman, Y. Barenholz, In vitro experiments showing enhanced release of doxorubicin from Doxil® in the presence of ammonia may explain drug release at tumor site, Nanomed. Nanotechnol. Biol. Med. 11 (2015) 1841–1850.
[46] J. Yu, X. Xie, M. Zheng, L. Yu, L. Zhang, J. Zhao, D. Jiang, X. Che, Fabrication and characterization of nuclear localization signal-conjugated glycol chitosan micelles for improving the nuclear delivery of doxorubicin, Int. J. Nanomedicine 7 (2012) 5079–5090.
[47] T. Fröhlich, D. Edinger, V. Russ, E. Wagner, Stabilization of polyplexes via polymer crosslinking for efficient siRNA delivery, Eur. J. Pharm. Sci. 47 (2012) 914–920.
[48] J.F. Marier, J.L. Brazier, J. Lavigne, M.P. Ducharme, Liposomal tobramycin against pulmonary infections of *Pseudomonas aeruginosa*: a pharmacokinetic and efficacy study following single and multiple intratracheal administrations in rats, J. Antimicrob. Chemother. 52 (2003) 247–252.
[49] A.-S. Messiaen, K. Forier, H. Nelis, K. Braeckmans, T. Coenye, Transport of nanoparticles and tobramycin-loaded liposomes in *Burkholderia cepacia* complex biofilms, PLoS One 8 (2013) e79220.
[50] L. Desigaux, M. Sainlos, O. Lambert, R. Chevre, E. Letrou-Bonneval, J.-P. Vigneron, P. Lehn, J.-M. Lehn, B. Pitard, Self-assembled lamellar complexes of siRNA with lipidic aminoglycoside derivatives promote efficient siRNA delivery and interference, Proc. Natl. Acad. Sci. U. S. A. 104 (2007) 16534–16539.
[51] N.F. Bouxsein, C.S. McAllister, K.K. Ewert, C.E. Samuel, C.R. Safinya, Structure and gene silencing activities of monovalent and pentavalent cationic lipid vectors complexed with siRNA, Biochemistry 46 (2007) 4785–4792.